PROCEEDINGS of the
23rd International Congress on Acoustics

9 to 13 September 2019 in Aachen, Germany

Determining the airborne sound insulation improvement of thermal cladding systems in combination with heavyweight exterior walls

Claire CHURCHILL[1]; Maximillian NEUSSER[2]; Simon HINTERSEER[3]

[1] TU Wien, Austria

[2] ACOM Research, Austria

[3] TU Wien, Austria

ABSTRACT

Prediction of the sound insulation (SI) of modern thermal insulation systems for exterior walls is considered. These products all have in common a lightweight insulating layer of primarily thermal function (which may consist of a porous or non-porous material), and a weatherproof finish; the systems measured in the laboratory included a grout and skim finish or a prefabricated cladding system. In all cases, a typical heavyweight exterior wall was cladded. Modern examples of such systems are ETICS (External thermal insulation composite systems) and curtain walls. In their simplest form, such cladding systems can be modelled as a spring-mounted mass. However, Austrian standards demand that the spring-mounted layer be combined with structural fixings. In the examined cases sparse distributions (up to 12 connections/m²) of point connections were used. The SI of simplified and typical thermal cladding systems (i.e. with and without structural fixings) were measured in an accredited laboratory facility and these results were compared with a calculation method to determine SI. The possibility of using established methods to determine the coupling loss factors in such combined systems was considered. The structural wall is of heavyweight construction, and the SEA problem can be simplified to a primary path analysis.

Keywords: SRI, thermal cladding, insulation

1. INTRODUCTION

Current state of the art to determine accurate sound insulation data for heavyweight thermally clad exterior wall systems in Austria is to methodically measure each system or to determine an airborne sound insulation improvement (1) (Annex B) and sum it with a base wall construction. The potential exists to establish a model that can predict the sound insulation (SI) of thermal insulation systems for exterior walls. Prerequisites of a prediction model are flexibility and general applicability; providing a planning tool with current data for modern systems. In the historical development of such systems, insulation thicknesses of between 40mm and 80mm (typical in the 1980s) have risen to more frequently used 200mm to 300mm thicknesses today, due to significantly higher thermal insulation requirements. Refurbishment can also include the application of thermal insulation to an exterior wall of an old building with the intention of improving building physics parameters and the added benefit of an enhanced architectural appearance.

All such systems have in common a typical heavyweight exterior wall cladded with a lightweight insulating layer (of primarily thermal function which may consist of a porous or non-porous material), and a weatherproof finish; This finish can be a grout and skim or a prefabricated cladding system. Modern examples of such systems are ETICS (External thermal insulation composite systems) and curtain walls. In their simplest form, such cladding systems can be modelled as a spring-mounted mass. However, in the real world, Austrian (2) (and European (3)) standards demand that the spring-mounted layer be

[1] Claire.churchill@tuwien.ac.at
[2] Maximilian.neusser@acom-research.eu
[3] Simon.hinterseer@tuwien.ac.at

combined with structural fixings.

The SI of simplified and typical thermal cladding systems (i.e. with and without structural fixings) were measured in an accredited laboratory facility and these results are compared with calculation methods to determine SI. The project work is framed by an underlying desire among participating manufacturers to augment a single-figure weighted sound-reduction index (R_W) with frequency-dependent data. The structural walls are all of heavyweight construction. The systems were measured in an accredited Austrian laboratory and were compared with simple modelling methods.

2. SAMPLE DESCRIPTIONS

A 320mm brickwork wall constructed from rockwool filled cellular brickwork was clad with 160mm expanded polystyrene (EPS) with varying detail. Two thickness of weatherproof layer were used and sparse distributions (up to 12 connections/m²) of point connections were considered. Five samples and the base wall were examined. The constructions are summarized in table 1.

Table 1 – Wall samples ([1]for this construction a calculated result only is presented)

Base wall	EPS thickness, mm	Render thickness, mm	Number of anchors, /m²
320mm cellular brickwork	--	--	--
320mm cellular brickwork	160	10.2	--
320mm cellular brickwork	160	3.9	--
320mm cellular brickwork	160	10.2	6
320mm cellular brickwork[1]	160	10.2	10
320mm cellular brickwork	160	10.2	12

To measure the acceleration level difference, small samples consisting of one EPS plate (dimensions 1000 mm x 500 mm) were attached to the brickwork wall and a thin layer of render <4.0mm was applied. Four small samples each with increasing percentage areas of adhesive covering were compared to assess the effect of differences in the glue layer. The coverings were 100%, 70%, 40% and 20% of the area of the EPS panel.

3. CALCULATION METHODS

3.1 Non-resonant path

The non-resonant path through the heavyweight wall was defined using (4):

$$\eta_{\mathrm{ij}} = \frac{c_0 S}{4\omega V_i} \frac{2\rho_0 c_0 K}{\omega(\rho_i \rho_j \omega^2 - K(\rho_i + \rho_j))} \tag{1}$$

Where c_0 is the speed of sound in air, S is the surface area of the wall, ω is the angular frequency, V_i is the volume of the adjacent room, ρ_0 is the density of air, K is the dynamic stiffness per unit area, ρ_i and ρ_j are the mass per unit area of the coupled plates. This formula is typically used to define an air spring but is equally applicable to any spring attached element to the wall. In this case, the spring stiffness of the resilient material layer and the spring stiffness of point (or line) fixings can be summed in parallel (4).

3.2 Resonant path

The resonant path was defined using a point connection model described in Hopkins (5) and Craik et. al. (6):

$$\eta_{\mathrm{ij}} = \frac{r_S}{\omega \rho_i} \frac{\mathrm{Re}\{Y_i\}}{\left|Y_i + Y_j + Y_c\right|} \tag{2}$$

Or an area spring defined by (7):

$$\eta_{\mathrm{ij}} = \frac{1}{\omega \rho_i} \mathrm{Re}\left\{\frac{1}{Y_j}\right\} \frac{|Y_c|^2}{|Y_i + Y_c|^2} \tag{3}$$

Where in each case r_s is the number of point connections per unit area Y_i and Y_j are the point mobilities of the plates and Yc is the connector stiffness defined by Hopkins (5):

$$Y_c = \frac{i\omega}{K} \tag{4}$$

Where K is the dynamic stiffness in the case of eqn. (2) or the dynamic stiffness per unit area in the case of eqn. (3). In the latter case, the spring stiffness of the resilient material layer and the spring stiffness of point (or line) fixings could be considered to act in parallel to sum the total stiffness. This allows for the wall covering to be attached by spring connections. An alternative expression for the resonant path was proposed by Neusser et. al. (8) from Vigran (9):

$$\Delta R = -10 \cdot \lg\left[\left(\frac{\omega_0}{\omega}\right)^4 + r\frac{\tilde{u}_{2.B}^2}{\langle \tilde{u}_1^2 \rangle}\sigma_{\mathrm{B,point}}\right] \tag{5}$$

Where ω_0 is the angular frequency of the mass-spring-mass resonance, r is the number of point connections, $\tilde{u}^2_{2,B}$ is the r.m.s velocity on the point connections, $\langle \tilde{u}^2_1 \rangle$ is the mean r.m.s velocity on the surface of the render and $\sigma_{\mathrm{B,point}}$ is the radiation efficiency of the plate due to the point connections given by Vigran (9):

$$\sigma_{\mathrm{B,point}} = \frac{2c_0^2}{\pi^5}\frac{1}{S}\frac{1}{\omega_c^2} \tag{6}$$

Where ω_c is the critical angular frequency of the plate. The second term in eqn. (5) is equivalent to Craik´s coupling loss factor between the heavyweight wall and receiving room (4):

$$\eta_{\mathrm{ij}} = \frac{2\rho_0 c_0^3 r}{\pi^3(\rho_i + \rho_j)^2 \omega} \tag{7}$$

One underlying assumption of eqns. (5) and (7) is an infinitely stiff connection between the heavyweight wall and the lining. It would therefore be conceptually incorrect to sum in parallel the spring stiffness of the point connectors in a calculation of non-resonant transmission as described in section 3.1 when using these methods. However, this possibility may not be completely excluded in the case of measured velocity level data (eqn. 5). A comparison of the methods was made and the results are shown in section 0.

3.3 Path analysis

An analysis is made using a "path-by-path" analysis which defines the energy level difference between two subsystems according to Craik (4):

$$\frac{E_1}{E_{\mathrm{n}}} = \frac{\eta_2 \eta_3 \ldots \eta_n}{\eta_{12}\eta_{23}\cdots\eta_{(n-1)\ n}} \tag{8}$$

Where η_i are the total internal loss factors and η_{ij} are the coupling loss factors. This is used to obtain the velocity level differences or sound reduction index respectively for comparison with measured results.

4. MEASUREMENT METHODS

4.1 Acceleration level difference

The acceleration level difference between the brickwork wall and the render on several small samples was measured using a shaker and pair of accelerometers. Three source positions and eight accelerometer positions per source were used. (It was not possible to excite one side of the wall with an airborne source because the measurements were not made in an enclosed space.) The shaker was attached to the opposite side of the brickwork wall from the samples using a screw thread and metal rawl plug. A MLS excitation signal was used. The accelerometers on the brickwork wall were attached to the wall on the same side as the small

samples. Only the acceleration level difference above 400Hz was of interest, therefore, the minimum distance between measurement positions, between the shaker source and measurement position, or between the measurement position and the edges of the sample was 100mm. A Norsonic 840 was used to acquire the level difference. The sample size was one EPS plate (dimensions 1000 mm x 500 mm).

4.2 Sound insulation measurement

The sound insulation was measured according to ISO 10140-2 (10) in an accredited test laboratory at TGM faculty of acoustics and building physics.

5. RESULTS

5.1 Velocity level difference

A comparison of measured and calculated velocity level difference is shown in Figure 1. (Note that the measured acceleration level difference is a ratio, and in this case may be used interchangeably with the velocity level difference (5).) Equations (3) and (5) are used to calculate velocity level difference across the whole frequency range. The amount of adhesive used to attach the EPS insulation affects the spread of the measured acceleration level difference especially in the vicinity of the mass-spring-mass resonance frequency, f_0. The collective standard deviations of the measured results are shown in Table 2.

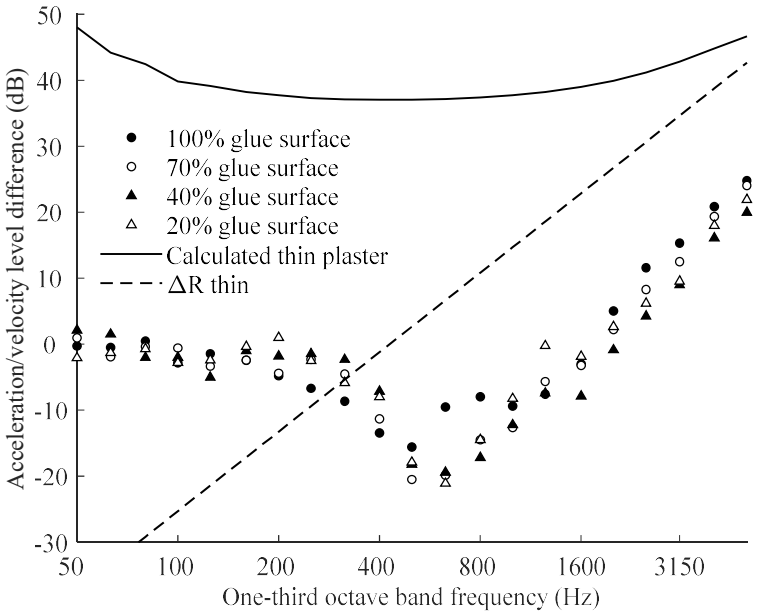

Figure 1 – Velocity level difference. The solid line '–' corresponds to the results obtained using eqn. (3) and the dashed line '--' to eqn. (5)

Table 2 – Combined standard deviations with 100%, 70%, 40% and 20% glue surface

Freq. (Hz)	315	400	500	630	800	1k	1.25k	1.6k	2k	2.5k	3.15k	4k	5k
s.d. (dB)	4.6	4.9	5.1	6.1	5.2	5.2	5.0	4.7	3.9	4.6	4.3	3.7	3.7

Agreement between measured and calculated results is poor at high frequencies (>630Hz) for a thin render (3.9 mm). This corresponds with poor agreement with SI in the model (see Figure 3). (Note that the dynamic stiffness of the EPS in the small samples is not yet verified.)

5.2 Sound insulation measurement (SI) and improvement (ΔR)

5.2.1 320 mm brick wall

The first step was to make a calculation for the base wall (320 mm brickwork). In the model the longitudinal wavespeed ($c_{L,p}$) of the brickwork was estimated to be 2300ms^{-1} (5) and the surface density of the brickwork (ρ) was calculated to be 231 kgm^{-2} from the mass of one block. The results from measurement and calculation are shown in Figure 2.

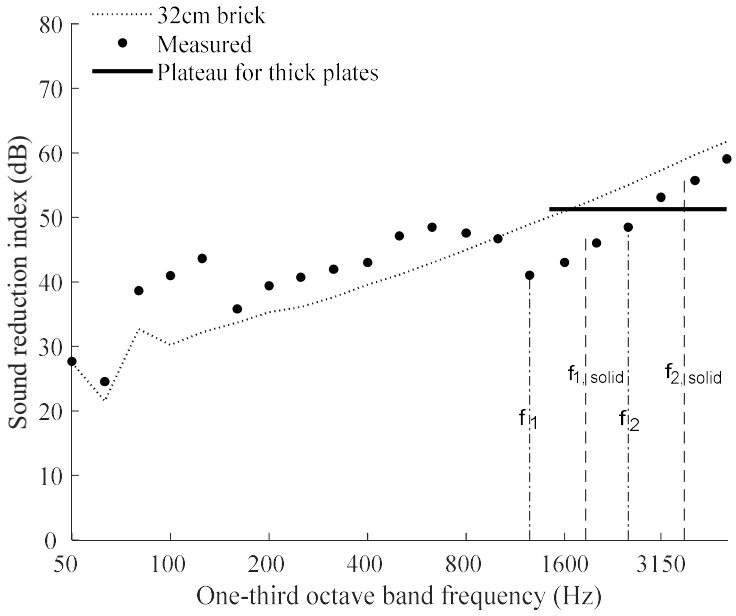

Figure 2 – 320 mm brick wall ($c_{L,p}$=2300ms^{-1}, ρ=231 kgm^{-2})

Agreement, within 6dB, is obtained between the calculation and measurement in the data ranges 50Hz-80Hz, 160Hz-1000Hz and 3150Hz-5000Hz. Poor agreement at high frequencies (>1000Hz) is likely due to thickness resonances of the wall. The calculated first and second thickness resonances, ($f_{1,solid}$ and $f_{2,solid}$) assuming solid brickwork are also shown in Figure 2. These do not correspond with the observed dip (f_1) and consequent supposed second thickness resonance (f_2). This could be because the blocks are not solid but are cellular and filled with rockwool. It could also be due to an incorrect estimate of Young´s modulus when making the calculation (which was determined using the estimated longitudinal wavespeed). The plateau for thick plates (calculated assuming solid brickwork) is also shown in Figure 2. However, a corresponding plateau in the measured data is not observed. The reason for poor agreement at 63Hz and 80Hz was not determined.

5.2.2 320 mm brick wall with 160mm EPS without point connections

The brick wall was cladded in 160mm EPS and a comparison between the results obtained with a thick (10.8 mm) and thin (3.9 mm) render was made. Measured and calculated results for a thick render are shown in Figure 3, and for a thin render in Figure 4. A sound insulation calculated using ΔR (eqn. (5)) is also shown in both figures by summing with the measured results for the 320mm brick wall. The value of the spring stiffness (K) of the EPS was modelled as 3.83x10^7 Nm^{-3} (the lower end of the measured values), the surface density (ρ) of the thick and thin render was measured to be 14.2kgm^{-2} and 5.4kgm^{-2} respectively and the longitudinal wavespeed ($c_{L,p}$) of the render was estimated to be 1610ms^{-1} (5). (Value for gypsum plasterboard used, although this may not reflect the actual material).

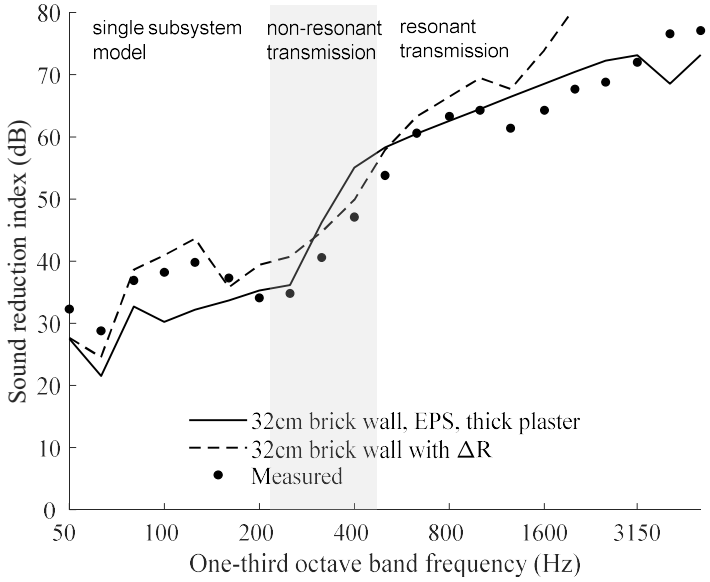

Figure 3 – 320 mm brick wall with 160mm EPS (K=3.83107 Nm^{-3}) and thick render ($c_{L,p}$=1610ms^{-1}, ρ=14.2 kgm^{-2})

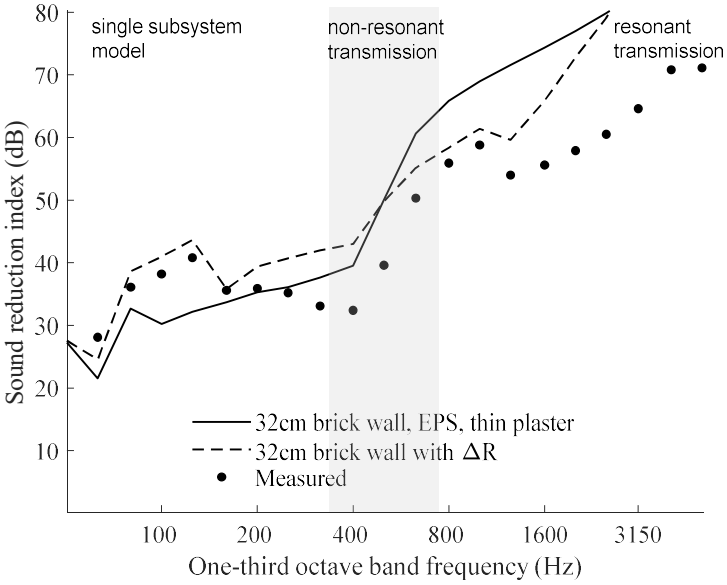

Figure 4 – 320 mm brick wall with 160mm EPS (K=3.83107 Nm^{-3}) and thin render ($c_{L,p}$=1610ms^{-1}, ρ=5.4 kgm^{-2})

Figures (3) and (4) show that sound insulation is divided into three frequency regions. A low frequency region, below the mass-spring-mass resonance, f_0, where the panel and lining is modelled as a single plate, a mid frequency region where Eqn. (1) is used to model non-resonant transmission and a high frequency region where Eqn. (3) is used to model the resonant transmission.

The model follows the general trend of the measured results for the thick render (Figure 3); although the values are not within 6dB at 63Hz, 100Hz, 125Hz, 315 Hz or 4000Hz. Poor agreement between the model and measurement for the thin render (Figure 4) at many frequencies is likely because the thin layer is no longer acting independently of the EPS and a combined material constant or some other model may be required. Therefore is a limiting render thickness (within the range 3.9 mm to 10.2 mm) can be assumed below which good agreement between measurement and calculation is not achieved. Sound insulation calculated using ΔR diverges significantly from the measured data at high frequencies (>1250Hz).

5.2.3 320 mm brick wall with 160mm EPS with point connections

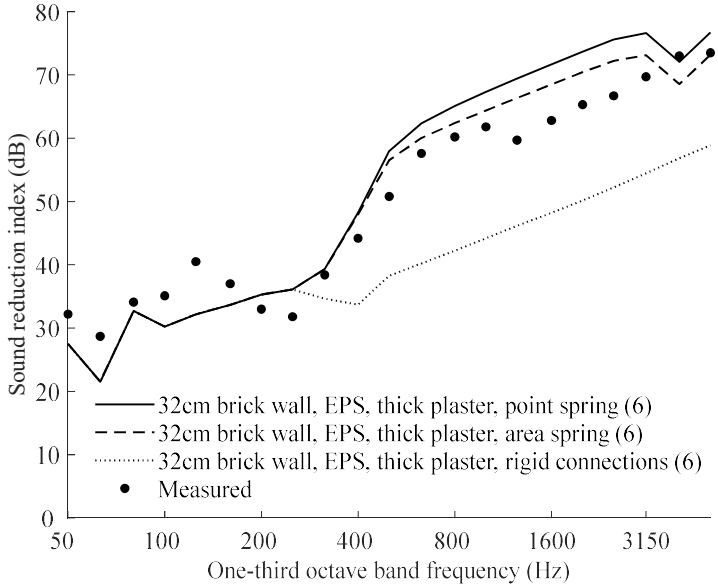

Figure 5 – 320 mm brick wall with 160mm EPS, thick render and 6 point connections. The solid line '–' corresponds to the results obtained using eqn. (2), the dashed line '--' to eqn. (3) and the dotted line '…' to eqn. (7)

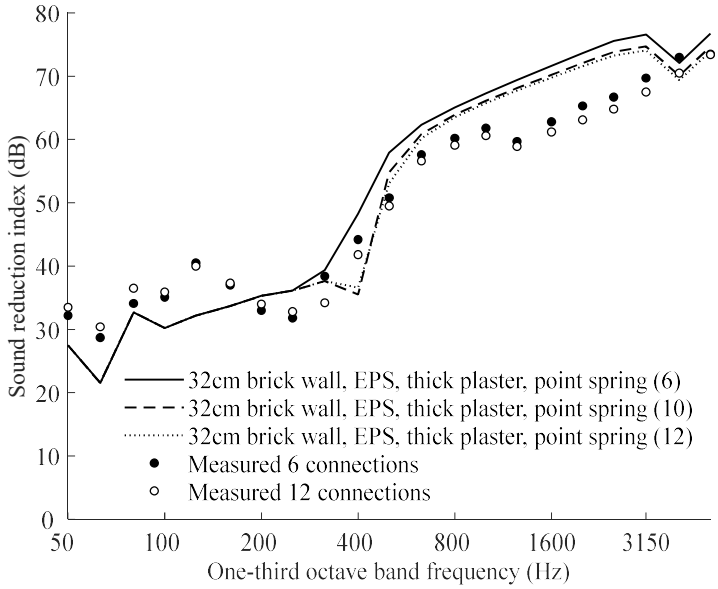

Figure 6 – 320 mm brick wall with 160mm EPS, thick render and 6, 10 or 12 point connections/m^2

Comparison of three models (eqns. (2), (3) and (7)) and measured data are shown in Figure 5. The area spring given by eqn. (3) agrees slightly better with measured data than point springs only (eqn. (2)). The rigid point connection model (eqn. (7)) gives significantly poorer agreement and the high frequencies therefore cannot be modelled by rigid point connections. Where required the spring stiffness of the point connections was estimated to be $4.0 \times 10^6 \mathrm{Nm}^{-1}$.

The effect of increasing the number of point connections for the point spring model is shown in Figure 6. The effect of a shifting upwards mass-spring-mass resonance can also be incorporated by summing the spring stiffness of the number of connectors per unit area in parallel together with the dynamic stiffness per unit area as described in Craik (4).

6. CONCLUSIONS AND FURTHER WORK

When modelling EPS cladding on brickwork exterior walls three distinct modelling regions can be identified: The low frequency region; where the cladding and wall can be modelled as a single system. The mid frequency region; where non-resonant transmission due to a mass spring mass resonance is observed. The high frequency region; where resonant transmission through the area and point springs from plate to plate is observed. The limit to which eqn. (3) can be applied to determine the resonant transmission is given by the render thickness and lies within the range 3.9 mm to 10.2 mm. Energy transfer via non-resonant and resonant paths through the system are governed by both the dynamic stiffness of the thermal insulation layer and the spring stiffness of the point connections.

A simultaneous measurement of velocity level on the heavyweight wall, the individual point connections and on the surface of the render could help to confirm the most appropriate way to model resonant transmission at high frequencies. These measurements could also be used to test whether eqn. (5), which makes use of a velocity level difference, can also be used in the case of spring connections. Measurements with a laser vibrometer could be used to determine the velocity ratio $\tilde{u}_{2.B}^2/\langle\tilde{u}_1^2\rangle$ which would allow different numbers of point connectors, r, to be added. Velocity level difference measurements could be repeated on a large sample in an enclosed space. Thus allowing a comparison between the level difference obtained with airborne and structural excitation. If the total loss factor of the render is measured a coupling loss factor between the brick wall and the render could also be calculated using the measured velocity level difference. The dynamic stiffness of the EPS in the small samples should also be verified. Finally it would be interesting examine a curtain walling system to determine if the same resonant and non-resonant loss factors can be used.

ACKNOWLEDGEMENTS

The work carried out this project, completed within an Austrian Collective Research - Funding project titled “Schall.Hoch.Bau”, was financed 40% by the commercial project partners and 60% by the FFG (Österreichische Forschungsförderungsgesellschaft).

REFERENCES

1. ISO10140-5. Acoustics -- Laboratory measurement of sound insulation of building elements. Part 5: Requirements for test facilities and equipment. International Organization for Standardization. 2010.
2. ÖNORM. B6400-1 Außenwand-Wärmedämm-Verbundsysteme (WDVS) Teil 1: Planung und Verarbeitung. 2017.
3. EN13499. Thermal insulation products for buildings - External thermal insulation composite systems (ETICS) based on expanded polystyrene - Specification. 2003.
4. Craik, RJM. Sound transmision through buildings using statistical energy analysis. s.l. : Gower, 1996.
5. Hopkins, C. Sound Insulation. s.l. : Elsevier, 2007.
6. Craik, RJM and Wilson, R. Sound transmission through masonry cavity walls. Journal of sound and vibration. 179, 1995, Vol. (1), 76-96.
7. Craik, RJM and Smith, RS. Sound transmission through lightweight parallel plates. Part II: structure-borne sound. Applied Acoustics. 61, 2000, 247-269.
8. Neusser, Maximillian, et al. Messung des Einflusses von Dübeln zur Befestigung von Wärmedämmverbundsystemen auf das Luftschalldämmmaß von Außenwänden in Massivbauweise. 2019.
9. Vigran, Tor Erik. Building Acoustics. s.l. : Taylor & Francis, 2008.
10. ISO10140-2. Acoustics -- Laboratory measurement of sound insulation of building elements -- Part 2: Measurement of airborne sound insulation. International Organization for Standardization. 2010.